Advances in Machinery, Materials Science and Engineering Application IX 791
M. Chen et al. (Eds.)

doi:10.3233/ATDE230542

Research on the Motion Mechanism of Polishing Machine Based on Joint Simulation

Mingsong ZHANG [a,1], Zhenyu CAI [a] and Jinzhi XIAO [b]
[a] *School of Machinery and Power, China Three Gorges University, Yichang, Hubei 443002 China*
[b] *Jiangxi Biotechnology Vocational College, Jiangxi Nanchang 330000 China*

Abstract. This paper for the mathematical modeling mechanism of the polishing machine, first based on the mechanical characteristics of the plate, analysis of the adhesive contact force and driving force, establish the polishing machine in the straight line, arc motion of kinematics and dynamic model, deduce the movement under the polishing machine movement speed, angular speed, position and driving friction force, driving moment. Finally, through joint simulation and verification by Admas and Simulink. The conclusion is that as the inclination of the wipe disc increases, the saturation speed of the linear motion will increase with a constant tolerance speed, the saturation angular velocity of the rotation motion also increases uniformly with the tolerance angular velocity. The rotational radius of the arc motion increases uniformly with the tolerance radius, and in the two sides of the disc inclination value in the opposite direction. On the contrary, the value decreases to the same value of the same direction and turns to the rotation movement. With the decrease of the disc rotation speed, the saturation velocity and saturation angular velocity of the line and rotation motion, the linear velocity and rotation radius of the arc motion are all decreasing, the angular velocity is increasing. This paper provides the theoretical basis for the steady state control of motion pose, and provides important reference for system parameter design and field construction of disc machine.

Keywords. Double-disc polishing machine, mechanical analysis, motion analysis, co-simulation

1. Introduction

Workers usually need to finish all night all pouring area, and poor construction environment, labor intensity, noise pollution is serious. Based on the pain points of the traditional construction operations, it is necessary to introduce the polishing machine to strengthen the control of the concrete pavement smoothness, so as to improve the pavement density, wear resistance and perception. Technology into the first to study polishing machine movement mechanism, master the polishing machine movement characteristics, discusses the control of the polishing machine construction movement strategy, the improvement of polishing machine, upgrade and as a subunit into the

[1] Mingsong ZHANG, Corresponding author, School of Machinery and Power, China Three Gorges University, Yichang, Hubei 443002 China E-mail: 592178236@qq.com.

cluster system has important significance, and will help to promote the development of road engineering cluster operation, makes our country in modern road engineering towards the world advanced level, enhance the international competitiveness of our infrastructure industry [1-5].

Literature [6] Conduct the path planning and design for the problems existing in the smooth process of the polishing machine. Literature [7] analyzes the driving mechanism of double-disc polishing machine, and studies the structural composition and working principle of the hydraulic system of polishing machine.

2. Force Analysis of the Polishing Machine

The main structure of the polishing machine studied in this paper is extended with disc polishing machine, with double disc polishing head. The structure diagram is shown in figure 1. It can be seen that under the action of heavy object m , the cement mortar deformation is the with displacement Δ_0 . Two plaster plates $A_1O_1B_1$、$A_2O_2B_2$ are parallel to the concrete floor, and respectively around the axis O_1C_1、O_2C_2 , rotation, turn the opposite, the speed is controlled by motor M at both ends, There are two electric push rods on both sides of the platform, which control the tilt Angle of the wipe plate and the axis around the center point C_1、C_2 respectively [8-11]. As shown in figure 2:

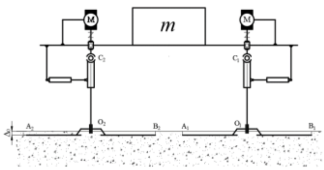

Figure 1. A schematic representation of the structure

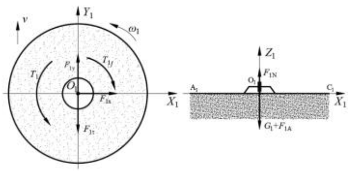

Figure 2. Schematic diagram of the wipe disk force .

The adhesive contact plays an important role in contact mechanics and tribology, as shown in figure 3, from the initial contact with the bulge (a), to the extrusion of the bulge to spread around (b), and finally the whole flattening of the plate and polishing of the bulge.

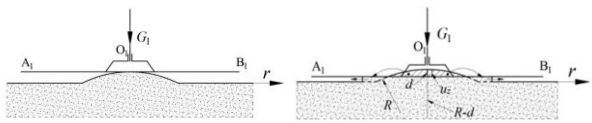

(a) Initial contact (b) Contact diffusion

Figure 3. Schematic diagram of the adhesive disk on the right.

The following are analyzed by uniform normal displacement method and Hertz pressure distribution method respectively, and the vertical displacement is respectively:

$$u_z = \frac{\pi p_0 a}{E^*}, u_z = \frac{\pi p_0 a}{4E^* a}(2a^2 - r^2), r \le a \tag{1}$$

Where E^* is the equivalent modulus.

Therefore, the pressure distribution based on the superposition principle and the vertical displacement is:

$$p = p_0\left(1-\frac{r^2}{a^2}\right)^{1/2} + p_1\left(1-\frac{r^2}{a^2}\right)^{1/2},\ u_z = \frac{\pi a}{E^*}\left[p_0 + \frac{1}{2}p_1\left(1-\frac{r^2}{2a^2}\right)\right] \quad (2)$$

Order Formula (1) is equal to formula (2), if:

$$p_1 = \frac{E^*}{\pi}\frac{2a}{R},\ p_0 = \frac{E^*}{\pi}\left(\frac{d}{a}-\frac{a}{R}\right) \quad (3)$$

γ_{12} is the relative surface energy density of the cement mortar and the plate material, and $\gamma_{12} = 2\sqrt{\gamma_1\gamma_2}$ and γ_1 is the surface energy density of the plate material steel, and γ_2 is the surface energy density of the cement mortar.On the total energy equation of the contact radius:

$$U_{\text{tot}} = E^*\left(\frac{8}{15}\frac{a^5}{R^2} + \frac{\gamma_{12}\pi a^2}{E^*} \pm \frac{4}{3}\frac{a^3}{R}\sqrt{\frac{2\gamma_{12}\pi a}{E^*}}\right) \quad (4)$$

Therefore, the final normal adhesion force F_A:

$$F_{\text{A}} = -\frac{3}{2}\gamma_{12}\pi R \quad (5)$$

The simplified tangential contact force is:

$$F_\tau = \mu F_{\text{N}}\left[1-\left(\frac{c}{a}\right)^3\right] \quad (6)$$

Finally, the size of the tangential contact force F_τ of the single wipe plate of the polishing machine is the same direction as the speed of the wipe disc v, that is, the tangential contact force is the driving gain force.

3. Study on the Dynamics of the Polishing Machine

3.1. Linear Dynamics

It is known that the mass of the polishing machine is m and evenly distributed on the left and right plate, with the inner and outer diameter of the plate R_1、R_2. In the stop state, the polishing machine wiping plate is subjected to the squeeze pressure of the cement mortar G and the normal adhesion F_A to produce the deformation. In the equilibrium state, the polishing machine moves the deflection Δ_t, that is,:

$$\Delta_t = \sqrt{\Delta_0^2 - \frac{1}{4}\left(R_1^2 + R_2^2\right)\theta^2} \tag{7}$$

The deformation depth δ of cement mortar from $P(r,\varphi)$ to the center of mass point O_2 on the bottom surface of the left plaster plate is:

$$\delta_1 = r_1\left|\theta_1\right|\cos\varphi_1, \quad \delta_2 = r_2\left|\theta_2\right|\cos\varphi_2 \tag{8}$$

The normal compressive stress distribution of the contact point $P(r,\varphi)$ at the bottom surface of the wipe plate can be further obtained as follows:

$$\sigma_{1P} = k\left(\Delta_{1t} + \delta_1\right), \quad \sigma_{2P} = k\left(\Delta_{2t} + \delta_2\right) \tag{9}$$

Thus, the velocity of the contact point $P(r,\varphi)$ can be summed by the forward velocity v and the tangential velocity v_τ :

$$\begin{aligned} \vec{v}_{1P} &= r_1\omega_1 \sin\varphi_1 \vec{i} + \left(v - r_1\omega_1\cos\varphi_1\right)\vec{j} \\ \vec{v}_{2P} &= r_2\omega_2 \sin\varphi_2 \vec{i} + \left(v - r_2\omega_2\cos\varphi_2\right)\vec{j} \end{aligned} \tag{10}$$

Further simplified, the projection results of the total friction $\vec{F}$ on the X and Y axes are as follows:

$$\begin{aligned} &\vec{F}_{1X} = 0, \ \vec{F}_{2X} = 0 \\ &\vec{F}_{1Y} = -D_1 v + E_1, \ \vec{F}_{2Y} = -D_2 v + E_2 \end{aligned} \tag{11}$$

μ is the dynamic friction factor between the plate and cement mortar.In formula:

$$\begin{aligned} D_1 &= \frac{\mu\pi k\,|\theta_1|\,(R_2 - R_1)}{w_1}\sqrt{\left(\frac{mg + 6\sqrt{\gamma_1\gamma_2}\pi R}{\pi k\,|\theta_1|\,(R_2^{\,2} - R_1^{\,2})}\right)^2 - R_2^{\,2} - R_1^{\,2}} \\ E_1 &= \frac{\mu\pi k\,|\theta_1|\,(R_2^{\,3} - R_1^{\,3})}{3} \end{aligned} \tag{12}$$

The same goes for D_2 and E_2.According to the result of Equation (12), the calculation result of the total friction applied on the right plate is equal to the total friction force on the left plate, namely:

$$\vec{F}_{1X} = \vec{F}_{2X} = 0, \vec{F}_{1Y} = \vec{F}_{2Y} \tag{13}$$

Therefore, the polishing machine does not synthesize friction in the X axis direction, but produces synthetic friction in the Y axis direction F_{fy} :

$$F_{fy} = -2D_1 v + 2E_1 \tag{14}$$

Further, the driving force F_{m} and the driving moment T_{m} of the polishing machine are deduced. As the friction force and the tangential contact force are equal and in direction, the combined torque cancel each other and the driving moment $T_{\mathrm{m}}=0$, and the driving force F_{m} is the resultant force of the friction force F_{fy} and the tangential contact force F_{τ}, namely:

$$F_{\mathrm{m}}=F_{f\mathrm{y}}+F_{\tau} \tag{15}$$

The extrusion stress F_{N} can be determined as:

$$F_{N}=2\pi k\Delta_{1t}(R_2^2-R_1^2) \tag{16}$$

The tangential contact force F_{τ} is inserted (18), and the final driving force F_{m} :

$$F_{m}=-2D_1v+H, H=2E_1+F_{\tau} \tag{17}$$

From equation (17), it is known that the polishing machine accelerates in the Y-axis direction, and the size of the driving force F_{m} decreases with the increase of the velocity v. When the force decreases and eventually reaches zero, the polishing machine speed also increases until it reaches the saturation speed v_s, namely:

$$v_{\mathrm{s}}=\frac{H}{2D_1}=\frac{|\theta_1|\omega_1\left(R_1^2+R_2^2+R_1R_2\right)}{3\Delta_t}+\omega_1\left(R_1+R_2\right)\left[1-\left(\frac{c}{a}\right)^3\right] \tag{18}$$

As can be obtained by equation (18), the saturation speed v_s of the motion of the straight line is only related to the rotation speed ω of the disc and the inclination θ of the disc. When the angular velocity is constant, the saturation velocity v_s is proportional to the inclination θ; when the dip is constant, the saturation velocity v_s is proportional to the angular velocity ω.

4. Simulation Validation

Polishing machine is between Simulink and Adams in the form of data flow implementation joint simulation, first in the UG software finish polishing machine geometric three-dimensional and conversion format import Adams software, then add joint constraint, setting drive, concrete contact force, finally the virtual prototype of polishing machine into mechanical system module, and import the Simulink environment and the mathematical model established comparison verification system [12]. Package the motion mathematical model and the mechanical system of the polishing machine respectively through the subsystem module [13-14].

In the comparison and verification system of the polishing machine, the linear motion, rotation motion and arc motion of the polishing machine are simulated and compared by adjusting the angular speed and inclination parameters of the polishing disc. Under the motion condition, the simulation time is 10s, the step length is 0.01s, set $w_1 = \pi$, $w_2 = -\pi$, $\theta_1 = 3^\circ$, $\theta_2 = -3^\circ$ in a straight line, arc motion setting $w_1 = \pi$, $w_2 = -\pi$, $\theta_1 = -1.5^\circ$, $\theta_2 = -3^\circ$, running the Simulink comparison and verification system. The signal obtains the position regularity curve and the velocity characteristic curve through the mechanical system and the theoretical model.

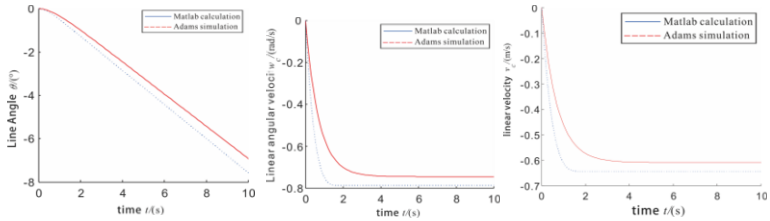

a) Comparison curve of rotation angle, angular velocity and linear velocity

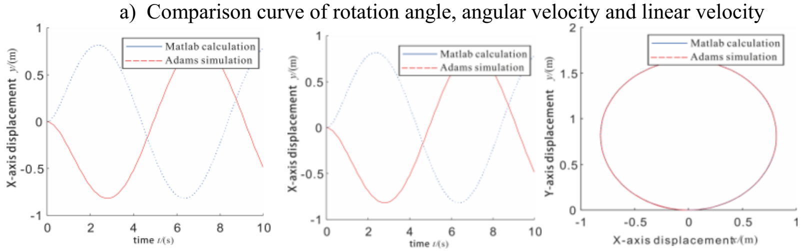

b) Comparcurves of X and Y axis displacement and path

Figure 4. Curcurve of arc motion.

Analysis figure 4, we know that the polishing machine follows the following motion change state: mathematical model and mechanical system in the simulation time $t = 0 \sim 4s$ and $t = 0 \sim 1.7s$ respectively. The instantaneous angular velocity ω_c increases with the driving moment and the linear velocity v_c increases with the driving force. The polishing machine makes the driving moment T_m and the tangential driving force $F_{m\tau}$ decrease in the centripetal force with time while the centripetal force F_{ma} increases with time. When $t = 4s$ and $t = 1.7s$, the driving force F_{m1} and F_{m2} reduced to the value equal to the tangential contact force F_τ, the driving torque T_m and the tangential driving force $F_{m\tau}$ reduced to zero, and the centripetal force F_{ma} increases with the instantaneous angular speed to saturation, reach a constant saturation speed $v_s = -6.1m/s$、$-6.4m/s$ and a constant saturation speed $\omega_s = -0.72\text{rad}/s$、$-0.79rad/s$, after which the polishing machine will keep the saturation speed and angular velocity, around the center of rotation $R_Z = 0.6m$ around the radius of rotation O_c.Observe the motion curve of the polishing machine, the speed and angular speed of the polishing are gentle, and the motion direction is the expected direction, which basically conforms to the process law of the rotation arc motion of the polishing machine.

5. Conclusion

In this paper, the adhesive contact force and the disc driving force are obtained by tribology. Analysis the motion of the polishing machine line and arc, and according to the mathematical model and the numerical results of the mechanical system, the numerical results of the polishing machine and the simulation of Adams mechanical system have corresponding offset, but the parameters change trend of the basic consistent, are within the reasonable range of the actual movement of the polishing machine, and the polishing machine movement curve also conforms to the expected movement mode. It therefore proves the correctness of the dynamics and kinematic modeling of the polishing machine in two motion modes. The theoretical results obtained in this paper can provide an important reference for the optimization design of system parameters and guide the field construction.

References

[1] Furiya H, Kiyohiro N. Floor polishing robot driven by self propulsive force. Journal of the Robotics Society of Japan. 1995; 13(6): 854-859.
[2] Kangari R, Yoshida T. Prototype robotics in construction industry. Journal of Construction Engineering and Management. 1989; 115(2): 284-301.
[3] Zhang ZF. Concrete surface polishing robot. Municipal Technology. 1998; (01): 58.
[4] Shin DH, Han DH. Open-loop velocity control of concrete floor finishing robots. Journal of Intelligent and Robotic Systems. 2003; 36(3): 285-300.
[5] Wang ZH, Chen Q, Zuo ZW, etc. Design and optimization of walking path of cast-in-place concrete polishing machine on bridge deck. Highway. 2021; 66 (07): 30-34.
[6] Huang ZH, Jiang JC, Liao XH. Design and simulation of hydraulic system of remote operation polishing machine based on AMESim. Machine Tool and Hydraulic Pressure. 2015; 43 (21): 179-182+185.
[7] Chen LW, Yan WF, Zhou Z. Four plate concrete polishing machine. CN: 209099129U, 2019-07-12.
[8] Popov. Principles of contact mechanics and tribology and its application. Tsinghua University Press, 2011.
[9] Qiu XY, Zhang JH, Yu W A rotating unit based on the walking mechanism of the remote control polishing machine. CN: 211772631U, 2020-10-27.
[10] Huang ZH, Liao XH, Jiang JC, et al. Analysis and research on the motion mechanism of driving polishing machine. Modern Manufacturing Engineering. 2016; (08): 151-156.
[11] Qiu XY, Zhang J, Yu W. A remote polishing spatula selection device. CN: 211775545U, 2020-10-27.
[12] Chen LP. Mechanical system dynamics analysis and ADAMS application tutorial. Tsinghua University Press, 2005.
[13] Nie GL, Bao YW, et al. Evolution law of the elastic modulus of cement mortar along with the temperature. Material Guide. 2019; 33 (02): 251-256.
[14] Ma LY, Tian CA, Song YX, et al. Experimental research on static, dynamic friction coefficient and elastic modulus of rock and cement mortar blocks under seismic conditions. Third National Conference on Rock Dynamics. 1992; pp. 61-68.